

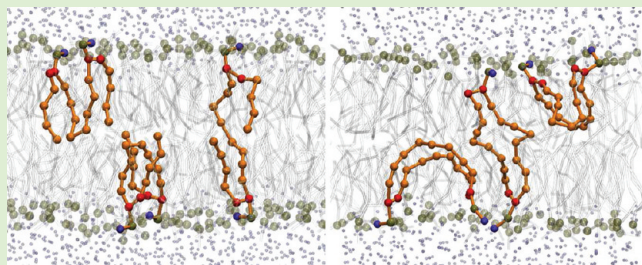
In Silico Design of Robust Bolalipid Membranes

Monica Bulacu, Xavier Périole, and Siewert J. Marrink*

Groningen Biomolecular Sciences and Biotechnology Institute and Zernike Institute for Advanced Materials, University of Groningen, Nijenborgh 7, 9747 AG Groningen, The Netherlands

 Supporting Information

ABSTRACT: The robustness of microorganisms used in industrial fermentations is essential for the efficiency and yield of the production process. A viable tool to increase the robustness is through engineering of the cell membrane and especially by incorporating lipids from species that survive under harsh conditions. Bolalipids are tetraether lipids found in Archaea bacteria, conferring stability to these bacteria by spanning across the cytoplasmic membrane. Here we report on in silico experiments to characterize and design optimal bolalipid membranes in terms of robustness. We use coarse-grained molecular dynamics simulations to study the structure, dynamics, and stability of membranes composed of model bolalipids, consisting of two dipalmitoylphosphatidylcholine (DPPC) lipids covalently linked together at either one or both tail ends. We find that bolalipid membranes differ substantially from a normal lipid membrane, with an increase in thickness and tail order, an increase in the gel-to-liquid crystalline phase transition temperature, and a decrease in diffusivity of the lipids. By changing the flexibility of the linker between the lipid tails, we furthermore show how the membrane properties can be controlled. A stiffer linker increases the ratio between spanning and looping conformations, rendering the membrane more rigid. Our study may help in designing artificial membranes, with tunable properties, able to function under extreme conditions. As an example, we show that incorporation of bolalipids makes the membrane more tolerant toward butanol.



INTRODUCTION

The lipid composition of biological membranes is critical for their function as a permeability barrier. This barrier should remain intact under conditions of environmental changes, such as fluctuations in temperature or exposure to hydrophobic and toxic substances. At the same time, the membrane should provide an optimal environment to support the activity of membrane proteins, like transporters and signaling proteins. These essential properties of membranes are governed by the lipid composition, which determines a variety of physicochemical parameters, including the lateral packing, fluidity, intrinsic curvature, bilayer thickness, and membrane surface charge. Partitioning of hydrophobic substances or toxic compounds into these membranes will affect all these parameters and thereby may lead to impaired membrane function and even to cell death. To counteract such effects and cope with relatively high concentrations of hydrophobic and toxic molecules, cells have developed a surprisingly diverse but still poorly understood ability to adapt their lipid composition.

Engineering of cell membranes takes this adaptation a step further and the ambitious goal is to engineer the cells in such a way that the cells become more resistant to external hydrophobic substances. The robustness of microorganisms used in industrial fermentations, for instance, is essential for the efficiency and yield of the production process and is to a large extent determined by the molecular architecture and composition of the cell envelope. A source of inspiration in designing new membranes can be found in already existing

ones that are known to remain stable and functional under extreme environmental conditions. Such membranes are found in, for example, Archaeabacteria and are considered to be the key ingredient in allowing these bacteria to survive in hostile habitats characterized by extremely high temperature, pressure or acidity.^{1–4} A special characteristic of some Archaea lipids is their occurrence as dimers, two conventional lipids with their carbon tails covalently joined together. This kind of dimeric, tetra-ether lipid is known generically as “bolalipid” or “bolaamphiphile” due to its similarity with an ancestral missile weapon named “bola” that consists of two weights attached at both ends of a rope.⁵ Depending on how the lipid tails are connected, the bolalipids are either cyclic (both tails connected) or acyclic (only one tail connection), as illustrated in Figure 1.

Membranes formed by bolalipids and by their mixture with monopolar lipids are known to have increased mechanical stability and lower permeability while retaining membrane fluidity.^{6–9} This is traditionally attributed to the fact that, in the lamellar phase, the bolalipids adopt predominantly a *trans* configuration (the two polar heads positioned in opposite membrane–water interfaces) in detriment of the *loop* configuration (both head groups located in the same membrane–water interface;^{4,10,11} see Figure 1). However, at

Received: October 17, 2011

Revised: November 20, 2011

Published: November 21, 2011



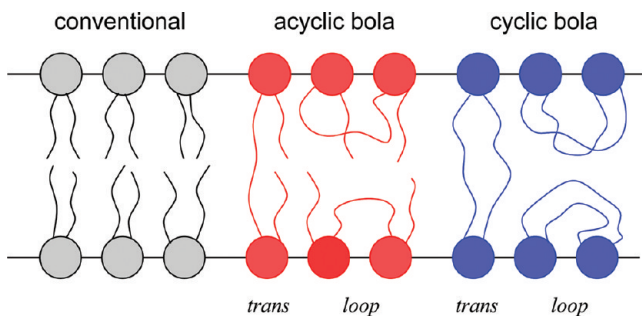


Figure 1. Schematic representation of conventional lipids (black) and of two types of bolaamphiphiles modeled in this paper: acyclic (red) and cyclic (blue) bolalipid. The horizontal lines indicate the position of the membrane–water interfaces.

this moment, there is no established method to absolutely determine the relative population of the *trans* and the *loop* configurations and no clear understanding of the relation between a preferred configuration and the structural and mechanical properties of the membrane. This is due to mainly two factors: bolalipids are very rare, natural ones are extracted with difficulty and at high price from cultured archaeal biomass (exceeding U.S. \$5000 per gram),¹² and only a reduced number of synthetic bolalipids analogues are available.^{13–20}

An effective and low-cost manner to study these lipids is to use computer simulations. The molecular dynamics (MD) technique, in particular, is highly suited because it allows for characterization of the membrane at the submolecular level.²¹

In this paper, we present results from MD simulations of model bolalipid membranes. The bolalipids are modeled as di-DPPC (dipalmitoylphosphatidylcholine) lipids connected either at one pair of chains (acyclic di-DPPC) or at both pairs (cyclic di-DPPC) by a short linker. Problematic, however, is the very slow dynamics of bolalipids, posing difficulties to a proper equilibration of the bolalipid membranes. To overcome the slow equilibration problem, we model the bolalipids at a coarse-grained (CG) level of representation using the MARTINI force field,^{22,23} which has proven very suitable for studying membrane properties in general.²¹ Following a self-assembly protocol,²⁴ bolalipid membranes are formed spontaneously. The self-assembled membranes are further equilibrated by creating a transient pore to allow the transfer between the *trans* and *loop* conformers. Having assured that the membranes are properly equilibrated, a process requiring multimicroseconds, we analyze the structural, dynamical, and mechanical properties of the bolalipid membranes, and explore the effect of the stiffness of the linker. In connection to the potential use of bolalipids to increase the robustness of membranes in fermentation processes, we also compare the butanol tolerance of bolalipid membranes with respect to normal lipid membranes. Our study should be viewed as a first step toward the *in silico* design of robust membranes, with potential applications in the field of biotechnology such as fermentation, drug delivery, sensors, and specialized receptor surfaces.²⁵

METHODS

Force Field Details. For representing our systems, we used the MARTINI coarse-grained model.^{22,23} In this model, groups of atoms (mostly four) are united into specific interaction centers that absorb all the molecular detail of the replaced atoms. By reducing the number of particles and the complexity of the interactions between them, longer simulation times can be achieved. This model is known to accurately

reproduce the structural and collective properties of many lipids (including DPPC) in the lamellar state.^{22,23,26–30} In the MARTINI model, each individual DPPC lipid consists of 12 coarse-grained particles: two hydrophilic (type “Q0” and “Qa”) modeling the choline and the phosphate moieties; two intermediately hydrophobic (type “Na”) for the glycerols; and eight hydrophobic particles (type “C1”), representing the 16 carbon-based units from the two lipid tails. Bolalipids are created by covalently linking the last tail beads of two pure DPPC lipids. Two cases are considered here: (i) only the *sn*-1 pair of tails is linked (acyclic di-DPPC), and (ii) both *sn*-1 and *sn*-2 tails are linked (cyclic di-DPPC). A schematic representation of the model is given in Figure S1 for the acyclic di-DPPC.

The aqueous phase is modeled by hydrophilic particles (type “P4”), each representing four real water molecules. All these coarse-grained particles interact via Lennard-Jones (LJ) potential with different well depth parameters depending on the specific pair type. The electrostatic interaction between choline (charge +e) and phosphate (charge -e) particles is modeled by a screened Coulomb potential, while the connectivity and stiffness of the molecules are modeled by a set of elastic bonds and harmonic bending potentials. Two additional harmonic bending potentials are considered for each link of the bolalipids (for the θ_1 and θ_2 angles from Figure S1), with the same equilibrium angle $\theta = 180^\circ$ and bending constant $K = 25 \text{ kJ mol}^{-1}$ as for the angles along the carbon tails. To model linkers with more flexibility, either one or both of these bending potentials were disregarded. We will refer to these systems as having semiflexible or flexible linkers, respectively. The standard linker (with two bending potentials per linker) is considered as stiff. For explicit details of the interaction parameters, we refer the reader to the original publications^{22,23} or to our Web site, <http://cgmartini.nl>, from which the bolalipid parameters used here can be downloaded.

System Setup. We have performed self-assembly simulations, followed by equilibration and production runs for six types of bolalipids: acyclic and cyclic, each with flexible, semiflexible, and stiff linkers. To characterize the self-assembly process, we have performed 200 independent simulations for each bola type, starting from different initial systems of 64 lipids randomly distributed in 2000 CG water particles (corresponding to 8000 real water molecules). After the self-assembly into the lamellar phase, we have selected five systems for each of the six bolalipid types and doubled their size by copying the simulation box in one of the directions parallel to the membrane plane. These membranes thus contain 128 bolalipids (note: 256 lipid heads). To equilibrate the membrane, the lipids have to interchange between the *loop* and the *trans* conformations, a process very similar to the “flip-flop” mechanism in conventional membranes, known to occur on the minutes to hour time scale.¹⁹ The lipid lateral diffusion is also significantly reduced compared to normal lipid diffusion.^{31,32} That is why, to date, the only MD studies reported have started from preassembled starting configurations with all the bolalipids in the spanning conformation, omitting the equilibration process.^{33–35} To fasten the bilayer equilibration, we use the mean field force approximation (MFFA)-boundary potential method developed by Risselada et al.³⁶ to create and maintain an artificial pore in the center of the self-assembled bilayers. The pore is induced and kept by a harmonic potential (force constant $150 \text{ kJ mol}^{-1} \text{ nm}^{-2}$) that repels all the lipid tail beads from a cylinder of 1.8 nm radius. The simulations with the pore were continued up to several microseconds until the ratio between the conformers is stabilized. Then, the pore was closed by removing the boundary potential and the simulations were continued for another 3 μs for further equilibration and system characterization. For comparison, we have also simulated preassembled acyclic and cyclic bolalipid membranes with lipids exclusively in the *trans* conformation, as in previous simulation setups,^{33–35} as well as a conventional DPPC bilayer.

Simulation Conditions. All the systems described in this paper were simulated using the GROMACS molecular dynamics package,³⁷ with a time step of $t = 20 \text{ fs}$. Standard simulation conditions as they apply to the MARTINI model were used.^{22,23} The Berendsen thermostat and barostat³⁸ were used to keep the temperature and pressure constant. The temperature was kept at 323 K for most of the

systems, except for the equilibration and production runs of some of the systems for which the temperature was increased to keep the bilayer in the liquid-crystalline phase. During the assembly and equilibration simulations, including the artificial pore, the pressure coupling was applied anisotropically to allow the initial cubic box to adapt to the membrane shape (with zero off diagonal coupling constants to keep the box rectangular). After equilibration, the pressure was controlled semi-isotropically (independently in the plane of the membrane and perpendicular to the membrane). The reference pressure was 1 bar in all directions.

RESULTS AND DISCUSSIONS

The results are presented and discussed in five subsections. The first two describe the self-assembly of the bolalipids into lamellar membranes and the subsequent equilibration of the membranes using an artificial pore. The last three sections describe the structural, dynamical, and mechanical properties of the bolalipid membranes. Six types of bolalipids are considered: cyclic and acyclic bolalipids with either stiff, semiflexible, or flexible linkers, all modeled as di-DPPC. In some cases, results are also compared to preconstructed bolalipid membranes with all lipids in a *trans* conformation and to a regular DPPC membrane.

Bilayer Formation through Self-Assembly. Starting with randomly distributed bolalipids in water we observed how, in the majority of the simulations, the lipids spontaneously self-aggregate into bilayers. This happens on a time scale of tens of nanoseconds, comparable to self-assembly times reported for conventional lipids.²⁴ A representative series of snapshots from the self-assembly process of the cyclic bolalipids with stiff linkers is shown in Figure 2.

In the self-assembled membranes the lipids assume both *trans* and *loop* conformations. The differentiation between the two conformations has been done by measuring the distance between the two heads of each lipid in the direction perpendicular to the bilayer: a *trans* conformation has been assigned for values bigger than 3 nm, a *loop* conformation otherwise. We have binned the fraction of lipids in the *trans* conformation, analyzing all 64 lipids in each of the 200 independent self-assembly simulations. The resulting histograms are shown in Figure 3 for each type of bolalipid membrane.

Most of the systems have more than 50% of the lipids in the *loop* configuration, that is, only few self-assembled systems have a prevailing *trans* population. The acyclic and cyclic bolalipids with semiflexible and flexible linkers self-aggregate in a very similar manner: on average, 70% of the lipids are in the *loop* configuration with a spread of around 10%. The stiff linker impedes the bolalipids to bend as much as the other types of linkers resulting in a slight increase in the *trans* population. This effect is more visible for the cyclic bola that has two linkers per lipid, approaching a 50% *trans* conformation. The low occurrence of *trans* conformations may seem surprising, given the general belief that bolalipids prefer the *trans* over the *loop* conformation. The origin of the large amount of looping bolalipids in the self-assembled membranes may be explained by the conformational preference of a single bolalipid prior to assembly: in the aqueous phase the lipid assumes a bended conformation (folding the tails together) rather than an extended one. Only the cyclic bolalipid with stiff linkers is observed occasionally in an extended conformation during the early stages of the self-assembly process.

After this analysis, we have selected 30 self-assembled membranes (five for each type of lipid), doubled their size, and continued the MD simulation to further equilibrate the

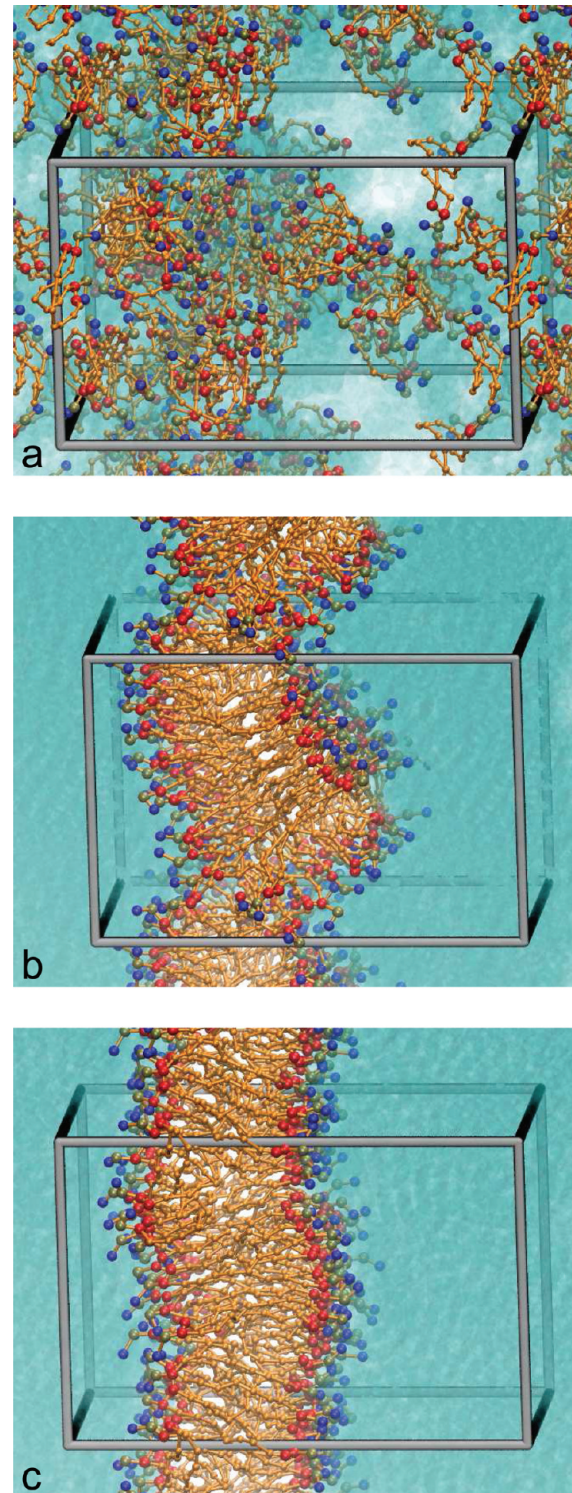


Figure 2. Bolalipids self-assembling into a bilayer membrane. The three snapshots are taken at $t = 1$ ns (a), 5 ns (b), and 20 ns (c) from a self-assembly simulation of 64 cyclic bolalipids, initially randomly placed in water. Lipids are depicted with orange tails, and blue/tan/red colored beads for the choline/phosphate/glycerol moieties. Water is shown as a blue haze.

systems. However, full equilibration proved problematic, as it would require lipid flip-flopping (i.e., the exchange of the lipid polar heads between the two leaflets). During several microseconds of simulation no change in the *trans* population has been noticed, in line with the experimental evidence for

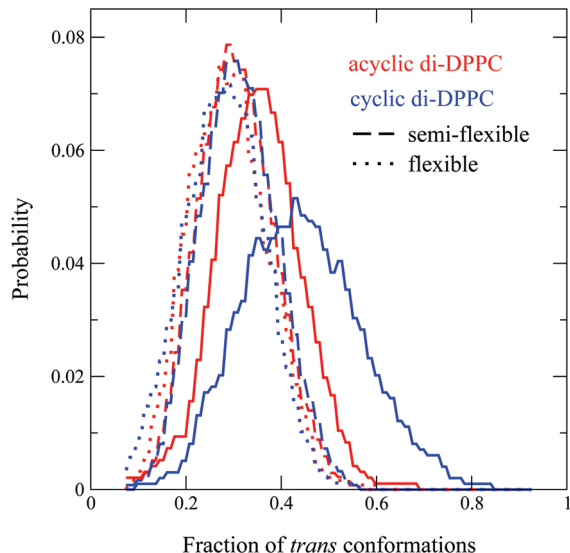


Figure 3. Fraction of *trans* conformations in self-assembled bolalipid membranes. Red color corresponds to acyclic bola and blue color to cyclic bola. The line type is related with the type of linker used to create the bolalipids: continue, stiff; dashed, semiflexible; dotted, flexible.

lipid flip-flop times of minutes to hours. We conclude that the self-assembled membranes are kinetically trapped into a nonequilibrium state and did not further analyze their properties.

Equilibration of the Trans/Loop Populations. To allow for the equilibration of the self-assembled bilayers, we introduced an artificial pore in the middle of the membranes. The pore provides a faster route for the lipid head-groups to move from one leaflet to the other by lowering the energy barrier for the *loop*—*trans* interconversion. This equilibration method has been proven successful in lipid vesicle equilibration in previous coarse-grained simulations.³⁶ In Figure 4, we show a particular, pore-mediated, flip-flop event observed for one of the cyclic bolalipids. The pore-mediated flip-flop takes place on a typical time scale of 10 s of nanoseconds.

During the equilibration of the membrane with the artificial pore, many such flip-flop events happen. Figure 5 shows the time evolution of the *trans* population for each of the six types of bolalipids, for a subset of the five independent simulations performed for each system. Similar convergence is observed for the remaining systems. The pore-mediated equilibration takes about 1 μ s for the acyclic bolalipids, while the cyclic bolalipids require about 4–5 μ s. After the flip-flopping into the *trans* conformation, most of the cyclic lipids adopt a gel-like state which slows down the system dynamics. To accelerate the equilibration of the cyclic bolalipids with stiff and semiflexible linkers, additional simulations were performed for these systems at an elevated temperature $T = 363$ K.

The equilibrium *trans* population evidently depends on both the bola architecture and on the linker stiffness. Upon removal of the pore boundary potential, this population increases slightly more due to the rearrangement of the lipids that were residing inside the pore. The final results for the *trans* population after pore closure are gathered in Table S1. The stiff acyclic and cyclic di-DPPC bilayers converge to $\approx 90\%$ of the lipids in the *trans* state. This outcome is consistent with a number of ^2H NMR studies on model bolalipid membranes,^{17,39–41} pointing to an overwhelming majority ($>90\%$)

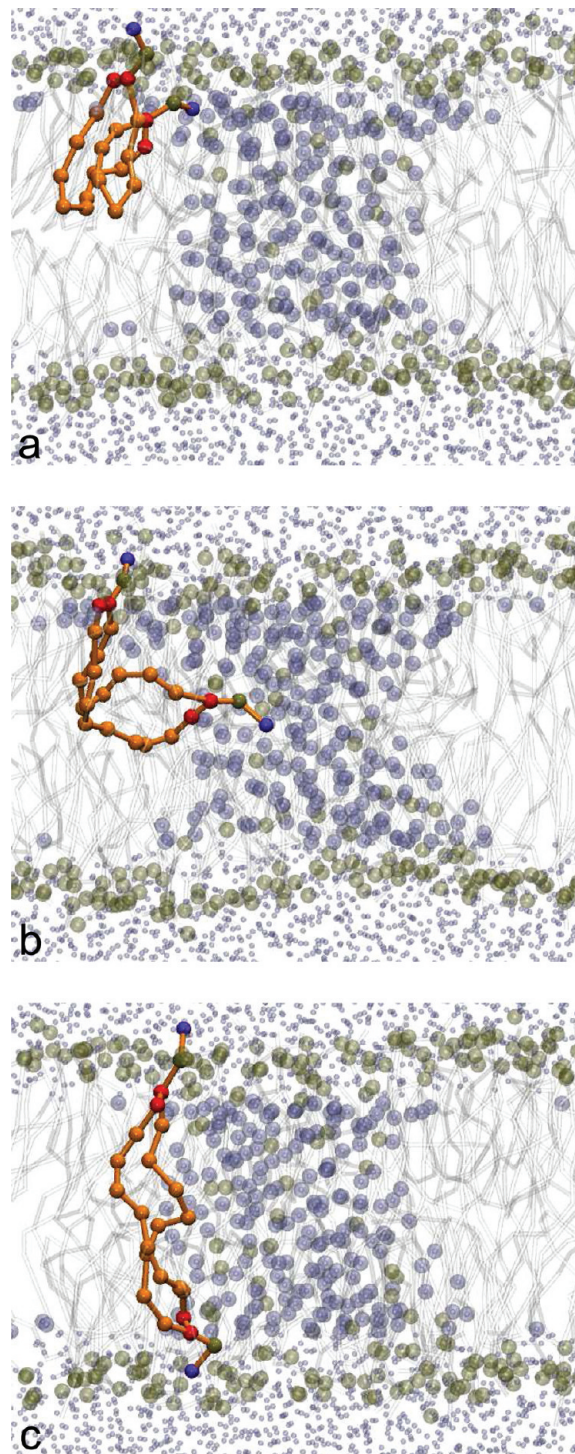


Figure 4. Pore mediated flip-flop of a bolalipid from *loop* to *trans* configuration. Snapshots at $\Delta t = 0$ (a), 5 (b), and 10 ns (c), taken from the equilibration of a self-assembled bilayer of cyclic di-DPPC (with flexible linker) using an artificial pore to allow lipid flip-flops. The membrane is represented in gray with the phosphate beads in transparent tan. The flip-flopping lipid is highlighted, using orange for the bonds and the methylene units, red for the glycerol, blue for the choline, and tan for the phosphate. The transparent blue beads represent the water phase. To make the pore visible, larger bead sizes have been used for the water inside the pore.

of the bolalipids in the membrane spanning configuration. For instance, di-DMPC bolalipids (very similar to the lipids simulated in our study) adopt a 9:1 *trans*/*loop* ratio in planar

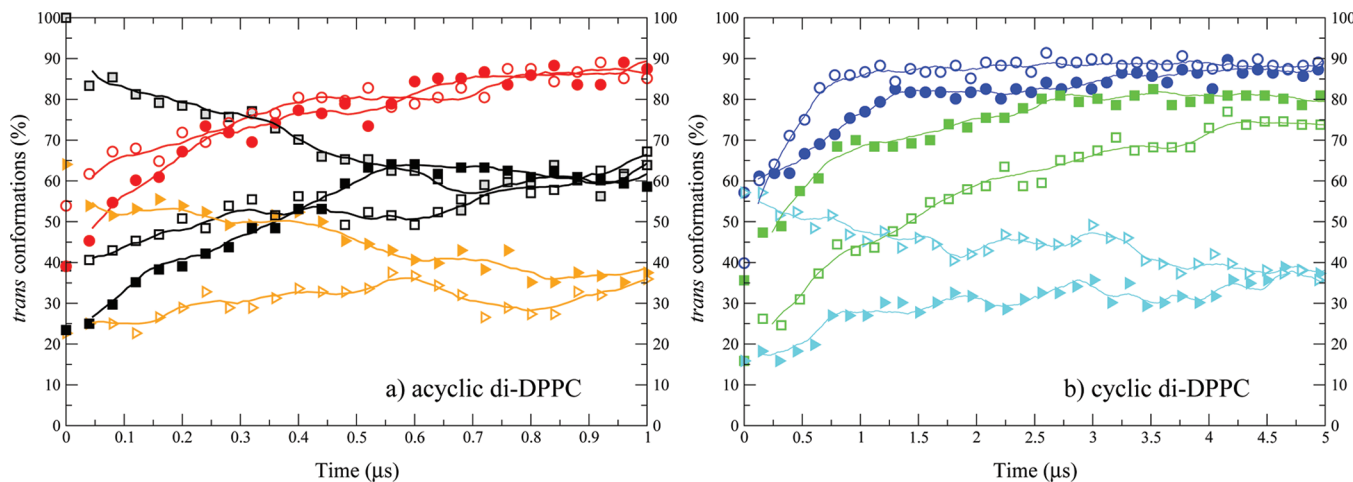


Figure 5. Time evolution of the transmembrane population during the equilibration of the bolalipid membranes in the presence of an artificial pore. Results for acyclic (left) and cyclic (right) di-DPPC membranes are shown. The symbols distinguish the linker flexibility: stiff, circles; semiflexible, squares; flexible, triangles. Different symbol filling is used to differentiate between independently simulated systems in the same class. The lines are running averages of the data.

bilayers,¹⁷ while ether bolalipids with 20 methylene units per unconnected tail (C_{20} BAS-PC) prefer almost exclusively the *trans* conformation.⁴⁰ The cyclic bipolar lipids extracted from Archaeabacteria are also assumed to adopt exclusively the *trans* conformation because the electron microscopy and X-ray techniques reveal monolayer membranes instead of conventional bilayer membranes.^{4,10,11}

By diminishing the linker stiffness the lipids are allowed to bend at lower energy cost, and therefore the *trans* population decreases to 40–60% (cf., Table S1 and Figure 5). The importance of the linker on the final distribution of conformers inside the membrane has been also revealed by experimental measurements. Investigating the flip-flop dynamics, Moss et al.¹⁹ measured a 60% *trans* probability in liposomes of phospholipid dimers cross-linked by a biphenyl group. In another study on dipolar phospholipids with a photoactive linker, using nonmembrane-permeating reagents, 50% of lipids in a *trans* configuration have been reported.¹⁶ Although these linking agents can not be directly compared to the type of linker investigated in our simulations, it is clear that a change of linker can tip the balance between predominantly *trans* and *cis* conformations.

After the pore closure, the membranes were further equilibrated for a period of 3 μ s. The analysis of the final 2 μ s of these simulations is presented in the next sections, separated into structural, dynamical, and mechanical properties of the membranes.

Structural Properties of Bolalipid Membranes. *Gel Phase Stabilized for Bolalipid Membranes.* A key characteristic of a membrane is the actual phase state of the lipids, which can be easily assessed through visual inspection of the systems. Representative snapshots of some of the equilibrated bolalipid membranes are shown in Figure 6. At the temperature of the simulations, $T = 323$ K, all of the acyclic bolalipids membranes are in a fluid phase (Figure 6a). The same is true for the cyclic bolalipid membranes with flexible linkers (Figure 6c). The cyclic systems with stiff and semiflexible linker, however, adopt a gel phase (Figure 6b) with the *trans* lipids neatly orientated parallel to each other in a tilted conformation. By performing additional simulations for some of the membranes over a fixed temperatures range, we have identified their gel phase transition

temperature. The approximate transition temperature is obtained from the observed kink in the dependence of membrane thickness on temperature (data not shown). For the acyclic bolalipids with the stiff linker the formation of the gel phase is observed around a temperature of 290 K, which is slightly above the transition temperature of 283 K for pure DPPC bilayers in the MARTINI model.²² This result is consistent with experimental evidence, indicating a small increase of the transition temperature of acyclic bolalipid membranes up to 20 °C in comparison with their corresponding standard monolipids.^{13,14,17} This temperature difference is reduced as the flexibility of the linker increases. In the case of cyclic bolalipids, the cross-linking of both lipid tails leads to much stronger effects on the gel–liquid phase transition temperature. Upon heating of the stiff cyclic membranes, melting is only observed at temperatures exceeding 375 K. Membranes formed by cyclic bolalipids with a semiflexible linker have a lower transition transition temperature $T \approx 355$ K, while for flexible linkers a value close to 300 K has been identified.

Density Distributions Show Disappearance of Slip Plane. Simulations studies allow the detailed characterization of the internal membrane structure via calculation of the density profiles. The density profiles of the lipid tail beads across the membrane are shown in Figure 7. Results for bolalipids with stiff linkers are shown only, and are compared to the profile for a normal DPPC bilayer. The bolalipid densities are decomposed into the contribution from the lipids in *trans* conformation and lipids in *loop* conformation. For both bolalipid types, the density increases and broadens compared to pure DPPC. The *trans* conformers induce a visible modification in the total density: the slip plane present in the center of the DPPC bilayer (as well as in many other conventional lipid bilayers) is reduced for the acyclic bolas and disappears completely in membranes of cyclic bolas. Note that the cyclic bolalipid membrane is in the gel phase, resulting in the almost flat density profile across the membrane.

The lipids in *loop* configuration, belonging to separate leaflets do not interdigitate in the middle of the membrane, remaining separated from each other like standard lipids do. However, looping conformations in each of the monolayers do show a

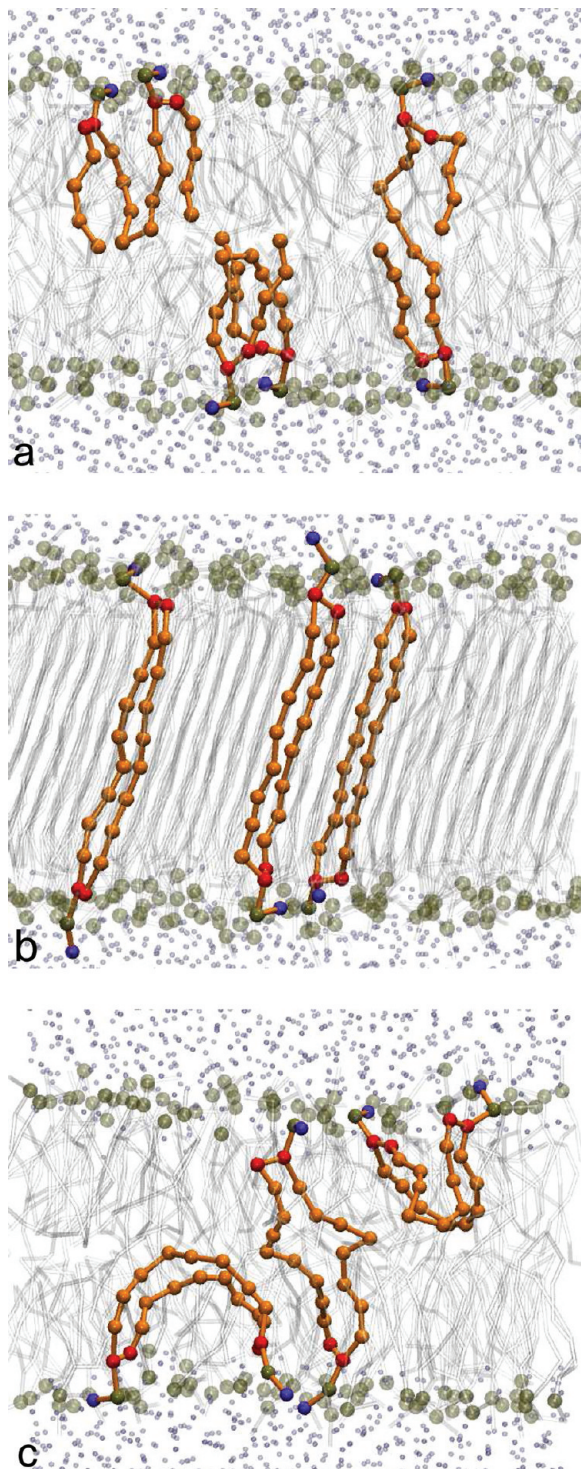


Figure 6. Molecular structure of equilibrated bolalipid membranes. The last snapshots from the simulations of stiff acyclic (a), stiff cyclic (b), and flexible cyclic (c) bolalipids, at $T = 323\text{ K}$, are depicted. The color code is identical to the one in Figure 4. Three lipids are highlighted to show representative *trans* and *loop* configurations (only *trans* for the stiff cyclic case).

preference to colocalize. In this way, two of them together act as a spanning lipid. No segregation between the lipids in *trans* and *loop* conformations was observed in any of the systems studied. The lipids adopting the *loop* configuration are also equally distributed between the upper or lower membrane leaflets.

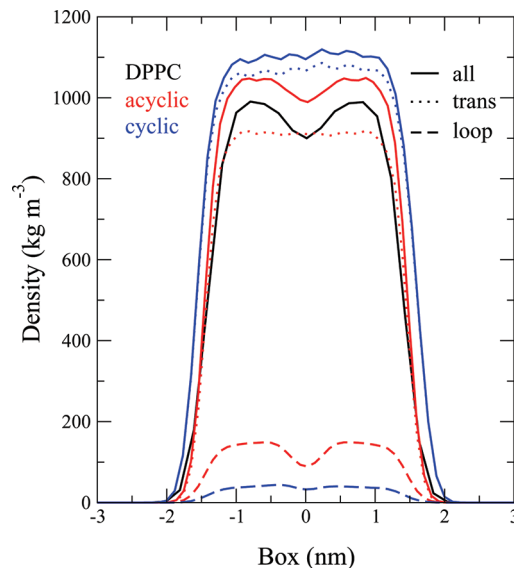


Figure 7. Comparison of the density distributions of the lipid tails obtained in standard DPPC membrane and bola di-DPPC membranes (stiff acyclic, red; stiff cyclic, blue). The lipid tail density for di-DPPC is decomposed into the contribution from the *trans* conformations (dotted lines) and *loop* conformations (dashed lines). The center of the membrane is taken at $z = 0$. The temperature is $T = 323\text{ K}$.

Bolalipids Have a Condensing Effect on the Membrane. Two important, and related, membrane properties are the bilayer thickness and area per lipid. The bilayer thickness d_{pp} has been determined as the distance between the peaks in the density of the phosphate moiety. The area per lipid was measured as the area of the simulation box in the direction parallel to the membrane, divided by half the number of lipid head groups. A remark should be made here: because the bolalipids have two head groups, we measure the area per headgroup to have a better comparison with the DPPC bilayer. All our results are gathered in Table S1. For reference, results for pure DPPC as well as for preassembled fully *trans*-di-DPPC membranes are also included. Two important trends can be observed. First, the bolalipid membranes are more condensed compared to their normal lipid analogues. The area per lipid headgroup decreases from 0.63 for normal DPPC to 0.60 for acyclic di-DPPC with stiff linkers, a 5% reduction. As a result of this condensation, the bilayer thickness increases by a similar percentage. The condensation of the cyclic bolalipid is even stronger, resulting in the actual transformation to a gel phase as discussed above. Second, the structural parameters are sensitive to the fraction of looping conformations. Comparing the self-assembled and preassembled acyclic di-DPPC membranes, with 90 and 100% *trans* conformers, the area per lipid decreases measurably, by almost 0.01 nm^2 . A more drastic effect is seen in the gel phase of the cyclic bolalipids, with a decrease of 0.07 nm^2 as a result of a change in the *trans* population from 96 to 100%. An increase in linker flexibility increases the fraction of looping conformers, and brings the area per lipid and thickness back toward the level of normal DPPC. Overall the results show that the presence of *trans* bolalipids lead to more condensed and thicker membranes compared to a standard DPPC bilayer. These trends are more evident in the case of cyclic di-DPPC lipids, in agreement with the simulation study of Shinoda et al.³⁴ for DPhPC (diphytanylphosphatidylcholine) and its analogous cyclic and acyclic bolalipids.

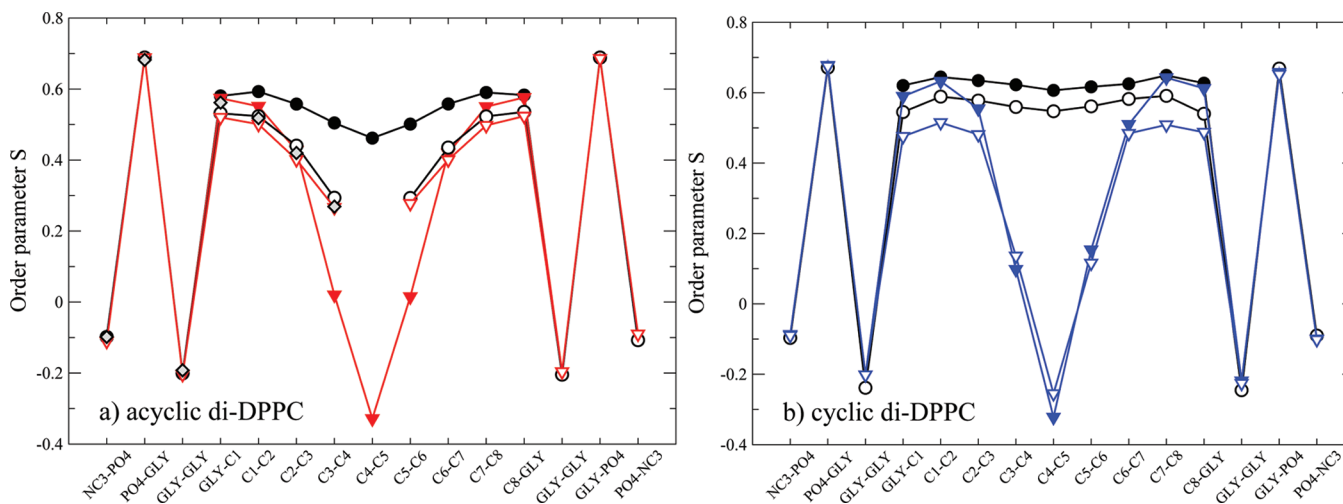


Figure 8. Order parameters for the lipid bonds with respect to the membrane normal for acyclic (left) and cyclic (right) di-DPPC. The black circles represent the lipids in *trans* conformation and red/blue triangles the lipids in *loop* conformation. The two tails *sn*-1 and *sn*-2 are differentiated by open and solid symbols, respectively. The order parameters for the reference DPPC bilayer are shown as gray diamonds in the left panel. All data are obtained at $T = 323$ K.

Order Parameters Point to Increased Order in Bolalipid Membranes. To characterize the bolalipid orientation within the membrane, we have computed the uniaxial order parameters S for all the bonds between the lipid coarse-grained particles:

$$S = \frac{1}{2} \langle 3 \cos^2 \theta - 1 \rangle \quad (1)$$

θ is the angle between the membrane normal and each individual bond and the averaging $\langle \rangle$ is done for all the lipids and over the entire simulation time. Perfect parallel alignment is indicated by $S = 1$, perfect perpendicular alignment by $S = -0.5$, while random orientation by $S = 0$.

For better understanding, we have also calculated the order parameters for *trans* and *loop* conformations separately, and distinguished between the *sn*-1 and *sn*-2 tails. The differentiation between the *trans* and *loop* bolalipid conformations due to their orientation within the membrane is used as a strategy to determine the *trans*/*loop* populations in bolalipid membranes by ${}^2\text{H}$ NMR spectroscopy.^{17,40,41} The order parameters for stiff acyclic and cyclic bolalipid membranes as well as for pure DPPC, all at $T = 323$ K, are shown in Figure 8. As expected, the effect of cross-linking of one or two pairs of tails is most evident in the lipid tails region. The headgroup bond order is actually unchanged compared to a normal DPPC bilayer. Overall, the order parameters for the tail region increase compared with DPPC, except for the cross-linked tails from the *loop* configurations which have to bend in the middle to allow positioning of their two heads in the same leaflet. This leads to a perpendicular orientation of the linker and its adjacent bonds with respect to the membrane normal and, consequently, to negative values for the order parameters. The cross-linked tails from the *trans* lipids have higher order parameters across the entire membrane, as an indication of their alignment parallel to the membrane normal. This effect is largest for the cyclic bolalipid, which is in the gel phase. Additionally, the data from Figure 8 display a significant difference between the two *sn*-1 and *sn*-2 tails. A small difference is known to exist also for DPPC but it seems that the cross-linking is increasing it. For

the acyclic bola, the unconnected (*sn*-1) tails behave as the DPPC tails, both in *trans* and *loop* conformations.

Dynamical Properties of Bolalipid Membranes. *Bolalipid Diffusion is Slow.* As characterized by the structural membrane properties, the bolalipid membranes are more packed compared with the standard lipid membranes. This is expected to reduce their lateral mobility inside the bilayer, with important effects on biomembrane functionality. To verify this, we have investigated the lateral diffusion of the lipids in the membrane plane. The lateral diffusion constant D has been calculated as the limiting slope of the mean-square displacement curve, using the Einstein relation for two-dimensional diffusion.

All our results are listed in Table S1. The diffusion coefficients for the acyclic di-DPPC are approximately five times smaller than for the pure DPPC at $T = 323$ K, irrespective of the linker stiffness. The cyclic lipids with stiff linkers, which are in the gel phase, are almost laterally immobile. In case of the preassembled cyclic membrane with all lipids in the *trans* state, the diffusion becomes unmeasurable low. The same is true for the cyclic bolalipids with semiflexible linkers. The self-assembled cyclic bolalipid membrane with semiflexible linker, however, is in the fluid phase at the elevated temperature of $T = 363$ K, due to the presence of a significant population of *loop* conformers. For this system, a comparable diffusion rate is found as for the acyclic bolalipids. Given the temperature difference, this means that diffusion rate in cyclic bolalipid membrane is even further reduced. The cyclic bolalipids with flexible linkers are still fluid at $T = 323$ K and also diffuse significantly slower than their acyclic analogues (by a factor of 2–3). This dissimilar dynamics between the acyclic and cyclic bolalipids is in good agreement with the limited experimental studies of bolaamphiphile diffusion.^{32,42}

Mechanical Stability of Bolalipid Membranes. Pressure Profiles. To characterize the bolalipid membranes from a mechanical perspective, we have calculated their lateral pressure profile along the bilayer normal. The lateral pressure profile, or stress profile, results from the inhomogeneous nature of the interactions within a membrane. As water, head groups, and acyl chains contribute through different forces, one finds the emergence of a nonuniform pressure distribution inside the

lipid bilayer. Elastic coefficients of membranes can be derived from the pressure profile,⁴³ and the profile itself has been proposed to be coupled to membrane structure and functionality.^{44,45}

The pressure profiles were calculated according to Lindahl and Edholm⁴⁶ and are shown in Figure 9 both for normal

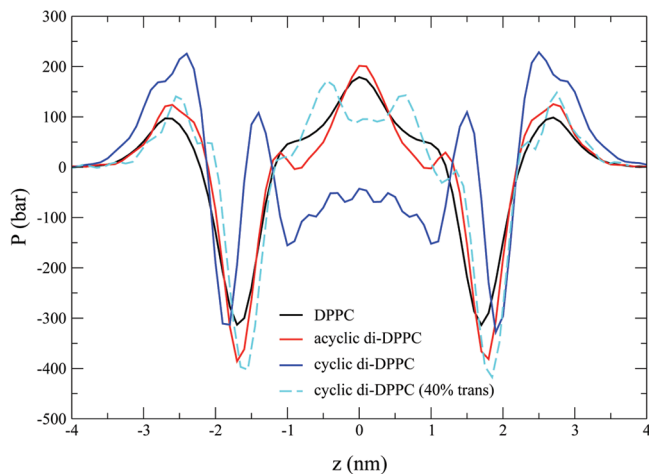


Figure 9. Lateral pressure profile across the membrane for DPPC (black), acyclic di-DPPC (red), cyclic di-DPPC with 100% (blue), and 40% *trans* population (cyan). All systems are at $T = 323\text{ K}$, with the exception of 100% *trans* cyclic di-DPPC, which is at the elevated temperature $T = 363\text{ K}$ (but still in a gel phase).

DPPC and di-DPPC membranes. Note, for clarity, we only present results for the preassembled membranes with stiff-linker bolalipids in the fully *trans* state as well as a self-assembled membrane of flexible cyclic bolalipids with a 40% *trans* population.

Comparing the normal DPPC membrane and the acyclic di-DPPC system, we see in both cases the characteristic W-shape of the pressure profile, arising from the interfacial tension between hydrophilic and hydrophobic regions and the opposing forces between headgroups and acyl tails. The differences are rather subtle, a somewhat increased repulsion in the headgroup region and a stronger attraction near the interface, which can be attributed to the smaller area per lipid of the acyclic bolalipid membrane with respect to normal DPPC (cf., Table S1). For the cyclic bolalipid membrane with 40% *trans* conformers, a somewhat different profile is observed. Additional peaks appear in the membrane interior next to the bilayer midplane, whereas the pressure in the center is significantly reduced. This shift in pressure can be understood by looking at the typical conformation of the looping bolalipids, see Figure 6 (panel c). Due to the bending, the linker region is located away from the bilayer center, giving rise to the additional peaks in the pressure profile. The profile for the fully *trans* cyclic bolalipid membrane is quite different, reflecting the gel state of the lipids. The neat packing of the lipid tails in the gel state, compared to the entropically confined tails in the fluid state, gives rise to a strongly reduced pressure in the middle.

In summary, the pressure distribution appears to be most sensitive to lipids in the *looping* conformation. Such unusual behavior has also been predicted theoretically by Mukhin and Kheyfets,⁴⁷ based on an elastic strings microscopic model to characterize membranes formed by cyclic bolalipids.

Bolalipid Membranes Show Increased Butanol Tolerance. The increased rigidity of bolalipid membranes suggests their potential use in applications where more resistant membranes are needed. For example, butanol molecules are toxic for most bacteria with standard membranes: high butanol concentrations disrupt the cell membrane and stop the cellular processes.⁴⁸ This limits the quantity of butanol resulting from fermentation and its production as biofuel at the industrial scale.

To find out if bolalipid membranes are more tolerant to butanol, we have performed additional simulations in which a fraction of the water molecules are replaced with butanol molecules in the equilibrated membrane systems. We mainly probed butanol/water fractions of 1/20, 1/10, and 1/5. Only the bolalipids with stiff linkers were considered. The temperature was kept at $T = 323\text{ K}$, except for the cyclic di-DPPC ($T = 363\text{ K}$). Similar to the observations reported in other simulation studies on small chain alcohols and monopolar lipid membranes,^{30,49–52} we observed the partitioning of butanol into the membrane/water interface. The butanol molecules preferentially reside near the glycerol region of the membrane (data not shown). Such localization leads to a lateral expansion of the membrane, which is linearly proportional with the butanol concentration; this is apparent from the plot of the area expansion with butanol concentration presented in Figure 10.

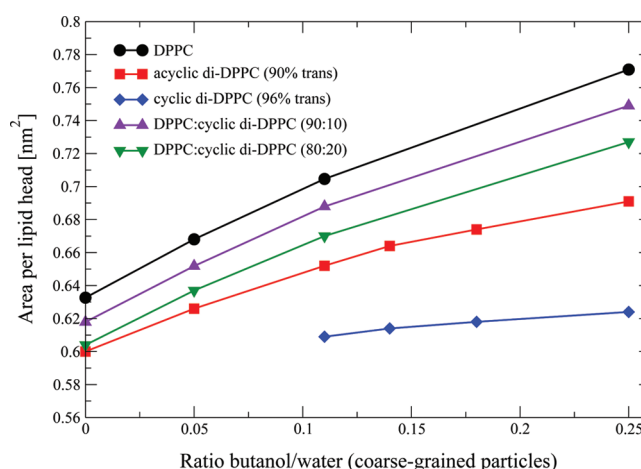


Figure 10. Area expansion of bolalipid membranes loaded with butanol. The area per lipid headgroup is shown for DPPC (black), acyclic di-DPPC (red), cyclic di-DPPC (blue), and mixtures of DPPC with cyclic di-DPPC in two ratios: 90:10 (violet) and 80:20 (green). The simulations have been performed at the temperature $T = 323\text{ K}$ with the exception of the pure cyclic bola ($T = 363\text{ K}$).

Ultimately, the continued loading of the membrane with butanol would lead to rupture of the membrane. Although we do not observe the actual rupture of the membrane, as our simulated membranes are artificially stabilized through the periodic boundary conditions, we can appreciate a clear difference between the expansion of a normal DPPC bilayer compared to the bolalipid membranes. The expansion of the bolalipid membrane (given by the slope of the curves in Figure 10) is almost 2-fold smaller for the acyclic case (a slope of 0.35 compared with 0.56 for pure DPPC) while for the cyclic bolalipids a slope of 0.11 has been obtained, even though the temperature in the latter case is higher. Concerning the cyclic bolalipids, we considered the expansion in the fluid regime

only; at a butanol fraction larger than 0.1 the cyclic bolalipid membrane undergoes a phase transition from the gel to the fluid state. Figure 10 contains also results for membranes formed by a mixture of DPPC and cyclic di-DPPC lipids, at two bola lipid concentrations of 10 and 20%. All the bolalipids are in the *trans* state. Due to the limited amount of bolalipids, these membranes are fluid at $T = 323\text{ K}$. In both cases, the lateral expansion of the membrane under the influence of butanol is significantly reduced compared to the pure DPPC membrane. Thus, our results suggest that doping of lipid bilayers with even a small fraction of bolalipids is already sufficient to make the membranes more tolerant toward toxic compounds such as butanol.

CONCLUSIONS

We presented results from molecular dynamics simulations of self-aggregation and equilibration of two bola amphiphile analogues, formed by two standard DPPC lipids with one and two covalent linkers between the tail ends. The equilibration of such systems, known for their extremely slow dynamics, was possible only by using a coarse-grained representation of the lipids and water, and in the presence of an artificial transient pore allowing equilibration of the *trans* and *loop* populations via lipid flip-flop.

Our results clearly indicate that, after equilibration, the bolalipids prefer the *trans* conformation (both polar head groups residing at opposite water–membrane interfaces) in detriment to the *loop* conformation (the polar groups are located at the same interface), consistent with experimental data. This arrangement naturally leads to a smaller area per polar headgroup and a larger thickness of the membranes compared with the conventional DPPC membranes. The order of the lipid tails is also increased and lateral diffusion slowed down.

We further showed that the fraction of *trans* conformers depends on the flexibility of the linker. A higher flexibility decreases the *trans* population due to the ability of the lipids to kink more and to adopt the *loop* configuration. As a result, membranes with different structural and dynamical properties are formed; in fact the nature and number of linkers allows for a tuning of the membrane properties all the way from almost identical to monopolar membranes, using very flexible linkers and acyclic bolalipids, to the very stiff and gel-like membranes formed with cyclic bolalipids and rigid linkers. Although our results pertain to pure bolalipid membranes, we expect, based on the strong effects we observed, even a limited fraction of bolalipids embedded in monopolar membranes to be able to modulate membrane properties. Thus, by incorporating certain types of bolalipids, an optimum can be found between robustness on the one hand, and fluidity on the other. As an example we showed the strong increase in tolerance of a bolalipid membrane toward a toxic substance such as butanol. Especially in the case of the acyclic di-DPPC bolalipid, the membrane is still in the biologically relevant liquid-crystalline phase, yet it can sustain twice the load of butanol compared to a conventional monopolar DPPC membrane. Likewise, a small fraction of cyclic bolalipids incorporated in an otherwise monopolar membrane showed a significant improvement toward butanol tolerance.

This is important for industrial fermentation processes, and may also be useful in lipid-based applications such as drug encapsulation and release. In the latter case, one could use the principle of a controllable linker (e.g., isomerization triggered

by light or changes in pH), acting as a switcher for the overall properties of the membrane.

ASSOCIATED CONTENT

Supporting Information

Figure S1 and Table S1. This material is available free of charge via the Internet at <http://pubs.acs.org/>.

AUTHOR INFORMATION

Corresponding Author

*E-mail: s.j.marrink@rug.nl

ACKNOWLEDGMENTS

We would like to thank Jelger Risselada and Martti Louhivuori for valuable discussions about the MFFA method and the pressure profile calculation. We are grateful for the computing time allocated by The Netherlands Computing Facilities (NCF) to perform part of the calculations presented in this paper.

REFERENCES

- (1) Koga, Y.; Morii, H. *Biosci. Biotechnol. Biochem.* **2005**, *69*, 2019–2034.
- (2) Benvegnù, T.; Brard, M.; Plusquellec, D. *Curr. Opin. Colloid Interface Sci.* **2004**, *8*, 469–479.
- (3) Benvegnù, T.; Lemière, L.; Cammas-Marion, S. *Eur. J. Org. Chem.* **2008**, *28*, 4725–4744.
- (4) De Rosa, M.; Gambacorta, A.; Gliozi, A. *Microbiol Rev.* **1986**, *50*, 70–80.
- (5) Fuoss, R. M.; Edelson, D. J. *J. Am. Chem. Soc.* **1951**, *73*, 269–273.
- (6) Elferink, M. G. L.; de Wit, J. G.; Driessens, A. J. M.; Konings, W. N. *BBA Biomembr.* **1994**, *1193*, 247–254.
- (7) Gliozi, A.; Relini, A.; Chong, P. L.-G. *J. Membr. Sci.* **2002**, *206*, 131–147.
- (8) Lemmich, J.; Hønger, T.; Mortensen, K.; Ipsen, J. H.; Bauer, R.; Mouritsen, O. G. *Eur. Biophys. J.* **1996**, *25*, 61–65.
- (9) Duwe, H. P.; Sackmann, E. *Phys. A* **1990**, *163*, 410–428.
- (10) Gliozi, A.; Rolandi, R.; De Rosa, M.; Gambacorta, A. *J. Membr. Biol.* **1983**, *75*, 45–56.
- (11) Elferink, M. G. L.; de Wit, J. G.; Demel, R.; Driessens, A. J. M.; Konings, W. N. *J. Biol. Chem.* **1992**, *267*, 1375–1381.
- (12) Bode, M. L.; Buddoo, S. R.; Minnaar, S. H.; du Plessis, C. A. *Chem. Phys. Lipids* **2008**, *154*, 94–104.
- (13) Runquist, E. A.; Helmckamp, G. M. Jr. *BBA Biomembr.* **1988**, *940*, 10–20.
- (14) Wang, G.; Hollingsworth, R. I. *J. Org. Chem.* **1999**, *64*, 4140–4147.
- (15) Kim, J.-M.; Thompson, D. H. *Langmuir* **1992**, *8*, 637–644.
- (16) Delfino, J. M.; Schreiber, S. L.; Richards, F. M. *J. Am. Chem. Soc.* **1993**, *115*, 3458–3474.
- (17) Cuccia, L. A.; Morin, F.; Beck, A.; Hebert, N.; Just, G.; Lennox, R. B. *Chem.—Eur. J.* **2000**, *6*, 4379–4384.
- (18) Svenson, S.; Thompson, D. H. *J. Org. Chem.* **1998**, *63*, 7180–7182.
- (19) Moss, R. A.; Fujita, T.; Okumura, Y. *Langmuir* **1991**, *7*, 2415–2418.
- (20) Raguse, B.; Culshaw, P. N.; Prashar, J. K.; Raval, K. *Tetrahedron Lett.* **2000**, *41*, 2971–2974.
- (21) Marrink, S. J.; de Vries, A. H.; Tieleman, D. P. *BBA Biomembr.* **2009**, *1788*, 149–168.
- (22) Marrink, S. J.; de Vries, A. H.; Mark, A. E. *J. Phys. Chem. B* **2004**, *108*, 750–760.
- (23) Marrink, S. J.; Risselada, H. J.; Yefimov, S.; Tieleman, D. P.; de Vries, A. H. *J. Phys. Chem. B* **2007**, *111*, 7812–7824.
- (24) Marrink, S. J.; Lindahl, E.; Edholm, O.; Mark, A. E. *J. Am. Chem. Soc.* **2001**, *123*, 8638–8639.

- (25) Mouritsen, O. G. *Life—as a matter of fat*, 1st ed.; Springer-Verlag: Berlin, 2005.
- (26) Marrink, S. J.; de Vries, A. H.; Harroun, T. A.; Katsaras, J.; Wassall, S. R. *J. Am. Chem. Soc.* **2008**, *130*, 10–11.
- (27) Kučerka, N.; Gallová, J.; Uhríková, D.; Balgavý, P.; Bulacu, M.; Marrink, S. J.; Katsaras, J. *Biophys. J.* **2009**, *97*, 1926–1932.
- (28) Kučerka, N.; Marquardt, D.; Harroun, T. A.; Nieh, M.-P.; Wassall, S. R.; de Jong, D. H.; Schäfer, L. V.; Marrink, S. J.; Katsaras, J. *Biochemistry* **2010**, *49*, 7485–7493.
- (29) Risselada, H. J.; Marrink, S. J. *Proc. Natl. Acad. Sci. U.S.A.* **2008**, *105*, 17367–17372.
- (30) Klacsová, M.; Bulacu, M.; Kučerka, N.; Uhríková, D.; Teixeira, J.; Marrink, S. J.; Balgavý, P. *BBA Biomembr.* **2011**, *1808*, 2136–2146.
- (31) Bruno, S.; Gliootti, A.; Cannistraro, S. *J. Phys. (Paris)* **1986**, *47*, 1555–1563.
- (32) Febo-Ayala, W.; Holland, D. P.; Bradley, S. A.; Thompson, D. H. *Langmuir* **2007**, *23*, 6276–6280.
- (33) Gabriel, J. L.; Chong, P. L. G. *Chem. Phys. Lipid* **2000**, *105*, 193–200.
- (34) Shinoda, W.; Shinoda, K.; Baba, T.; Mikami, M. *Biophys. J.* **2005**, *89*, 3195–3202.
- (35) Nicolas, J. P. *Lipids* **2005**, *40*, 1023–1030.
- (36) Risselada, H. J.; Mark, A. E.; Marrink, S. J. *J. Phys. Chem. B* **2008**, *112*, 7438–7447.
- (37) van der Spoel, D.; Lindahl, E.; Hess, B.; Groenhof, G.; Mark, A. E.; Berendsen, H. J. C. *J. Comput. Chem.* **2005**, *26*, 1701–1718.
- (38) Berendsen, H. J. C.; Postma, J. P. M.; van Gunsteren, W. F.; DiNola, A.; Haak, J. R. *J. Chem. Phys.* **1984**, *81*, 3684–3690.
- (39) Nakatani, Y.; Yamamoto, M.; Diyizou, Y.; Warnock, W.; Doll, V.; Hahn, W.; Milon, A.; Ourisson, G. *Chem.—Eur. J.* **1996**, *2*, 129–138.
- (40) Holland, D. P.; Struts, A. V.; Brown, M. F.; Thompson, D. H. *J. Am. Chem. Soc.* **2008**, *130*, 4584–4585.
- (41) Brownholland, D. P.; Longo, G. S.; Struts, A. V.; Justice, M. J.; Szleifer, I.; Petrache, H. I.; Brown, M. F.; Thompson, D. H. *Biophys. J.* **2009**, *97*, 2700–2709.
- (42) Kao, Y. L.; Chang, E. L.; Chong, P. L.-G. *Biochem. Biophys. Res. Commun.* **1992**, *188*, 1241–1246.
- (43) Safran, S. A. *Statistical Thermodynamics of Surfaces, Interfaces, and Membranes*; Addison-Wesley: Reading, MA, 1994.
- (44) Cantor, R. S. *J. Phys. Chem. B* **1997**, *101*, 1723–1725.
- (45) Brown, M. F. *Chem. Phys. Lipids* **1994**, *73*, 159–180.
- (46) Lindahl, E.; Edholm, O. *J. Chem. Phys.* **2000**, *113*, 3882–3893.
- (47) Mukhin, S. I.; Kheyfets, B. B. *Phys. Rev. E* **2010**, *82*, 051901.
- (48) Baer, S. H.; Bryant, D. L.; Blaschek, H. P. *Appl. Environ. Microbiol.* **1989**, *55*, 2729–2731.
- (49) Griepernau, B.; Leis, S.; Schneider, M. F.; Sikor, M.; Steppich, D.; Bockmann, R. A. *Biochim. Biophys. Acta* **2007**, *1768*, 2899–2913.
- (50) Dickey, A. N.; Faller, R. *J. Polym. Sci., Part B* **2005**, *43*, 1025–1032.
- (51) Kranenburg, M.; Smit, B. *FEBS Lett.* **2004**, *568*, 15–18.
- (52) Patra, M.; Salonen, E.; Terama, E.; Vattulainen, I.; Faller, R.; Lee, B. W.; Holopainen, J.; Karttunen, M. *Biophys. J.* **2006**, *90*, 1121–1135.